OBJECT RECOGNITION USING MOMENTS

OF THE SIGNATURE HISTOGRAM

by

Dustin G. Coker, B.S., B.A.

A thesis submitted to the Graduate Council of
Texas State University in partial fulfillment
of the requirements for the degree of
Master of Science
with a Major in Computer Science
May 2017

Committee Members:

Dan E. Tamir, Chair

Byron Gao

Yijuan Lu

FAIR USE AND AUTHOR'S PERMISSION STATEMENT

Fair Use

Duplication Permission

ACKNOWLEDGEMENTS

I would first like to acknowledge my thesis advisor Dr. Dan Tamir for his assistance in completing this work. His support and guidance have been remarkable. I cannot thank him enough for his patience and especially his good humor during this process. His commitment to helping students is an inspiration and I am eternally grateful for everything he has done for me personally.

I'd also like to thank Dr. Byron Gao. I am extremely thankful for not only his participation as a member of my thesis committee but also for his help and guidance during my initial graduate work.

I thank Dr. Yijuan Lu for participating as a member of my thesis committee and her helpful suggestions and instruction.

Finally, I would also like to thank my family, especially my wife, Nova. I could not have done this without her support and sacrifice. She is the light of my life and my best friend. My daughters, Zoey and Scarlet, have been my inspiration. Their laughter is medicine. My girls are my everything. Thank you.

TABLE OF CONTENTS

Page

LIST OF TABLES

Table **Page**

LIST OF FIGURES

Figure **Page**

ABSTRACT

The amount of digital information generated each day is increasing at a very high rate. Our ability to understand and make sense of such large amounts of unstructured data depends on efficient and reliable methods to automate analysis and classification. Still and motion imagery make up a large part of this ever expanding digital universe and therefore methods that target images and video data are increasingly important. The field of image processing has grown to meet this demand and, in particular, techniques for recognizing objects are playing a central role in this field.

Digital image processing is a continuum of processes and procedures. This paper is concerned with mid-level image processing, involving segmentation of an image into regions or objects, description of those objects, as well as recognition, and classification of those objects. Specifically, techniques and methods to recognize individual objects in images are investigated.

The goal of this thesis is to address the problem of analyzing and matching image objects. To achieve this goal, the use of statistical moments of the object signature is investigated. An object signature is derived by taking the Euclidean distance from the centroid of the object to every pixel on the boundary of the object. A relative frequency histogram is constructed from the object signature and then used to approximate a probability density function for the signature. Statistical moments are

then applied to the histogram to generate a novel set of descriptors that are invariant to rotation, translation, and scaling.

Existing techniques that utilize moments of the entire image are examined along with moments applied to just the object contour. Additionally, the use of two-dimensional Fourier Descriptors applied to the object contour are considered as well as one-dimensional Fourier Descriptors applied to the object signature. Finally, moments applied directly to the object signature are investigated. Experiments are performed to evaluate and compare these techniques with the method introduced in this work. Recognition accuracy as well as the quality of recognition are used to differentiate between the various techniques.

The results of the experiments show the method introduced in this work, statistical moments of the histogram of the object signature, proves to be a viable alternative to the other methods discussed. In particular, since only the center bin-values of the constructed histogram are used to calculate moments, the computational costs are orders of magnitude smaller than the computational cost of other methods considered in this thesis. In addition, the effect of binning the data when constructing the histogram compensates for noise introduced by scaling and rotation, resulting in an improvement in the quality of recognition over several of the other methods investigated.

I. INTRODUCTION

The International Data Corporation estimates that by 2020, 40 zettabytes of digital information will have been generated. With the increasing use of connected smart devices, embedded systems, and sensors, it is expected that most of that information will be in the form of unstructured data, such as video and images. Consequently, there is an ever-growing need to automate the analysis of this type of data, i.e. still and motion imagery. The use of computers to extract meaningful information from images and video is indispensable as we try to understand our digital universe.

The types of digital images generated today, range from electron microscopy of bacteria to “selfies” posted on Facebook. They span an enormously large range of the electromagnetic spectrum, from gamma rays to radio waves, and processing these images involves different techniques and methods. The science of Digital Image Processing has grown to meet this demand. This paper focuses on methods to describe the constituent parts or objects of an image in a way that facilitates recognition and differentiation between them. A good example of this process is the modern toll road. Many newer toll roads no longer employ tollbooths but rather use cameras to take pictures of license plates. The individual letters and numbers of the license plate are identified and a bill sent to the registered owner.

This thesis addresses the problem of analyzing and matching objects in images. The proposed solution is to use moments of the histogram of the object signature. Six experiments are performed. The first experiment considers a set of seven moment-invariant descriptors. The application of those descriptors to just the object contour is then examined. Next, the use of two-dimensional Fourier descriptors applied to the object contour and one-dimensional Fourier descriptors applied to the object signature is investigated. The use of mathematical moments to describe the object signature is considered and finally, taking moments of the histogram of the object signature is examined. The accuracy of each method in recognizing image objects is compared along with the quality of that recognition.

The hypothesis of this thesis is that taking moments of the histogram of the object signature is more efficient and more accurate than the other methods discussed for object recognition.

The contribution of this research is a novel method for recognizing objects in images. The method utilizes a minimum number of moments of the histogram of the object signature, and due to the fact that only the center bin-values of the histogram are used in calculating the moments, the number of computations required are orders of magnitude smaller, resulting in effective, accurate descriptors. Whereas other authors have applied moments to the entire image or directly to the contour or the object signature, no one has investigated applying moments to the histogram of the object signature.

This paper is organized as follows: Chapter 2 gives an introduction to Digital Image Processing concepts and provides the necessary background for this research. The object signature is defined along with histogram, mathematical moments, and Fourier descriptors. Chapter 3 is a literature survey that describes the relevant research. Chapter 4 outlines the experimental setup used to compare and evaluate the various methods and techniques for object recognition. Chapter 5 includes the results of the experiments and in Chapter 6 the results are analyzed. Chapter 7 presents a conclusion of our efforts and highlights future research.

II. BACKGROUND

2.1 Image Processing

Digital image processing is a continuum of processes and procedures. Lower level procedures are concerned with primitive operations designed for preprocessing the image. Mid-level image processing involves segmentation of an image into regions or objects, description of those objects, recognition, and classification of individual objects. At the highest level, processing consists of interpretation of recognized objects [1]. This paper is concerned with mid-level processing, specifically techniques and methods to recognize individual objects in a segmented image.

2.1.1 Images

An image is represented by a two-variable function, $f(x, y)$, where x and y are coordinates in the Cartesian plane. This function defines the intensity, or grey-level, of the image at any pair of coordinates as follows:

$$I = f(x, y) \tag{1}$$

If the quantities x, y, and I are all discrete, the image is a digital image. A digital image is composed of a finite number of picture elements, or pixels, each with

discrete location (x, y) and discrete intensity I. In a binary image, the pixels only take on one of two values, for example zero or one [1]. In this thesis, only binary images are considered.

2.1.2 Neighbors

For pixels with coordinates (x, y), the set of 4-neighbors is defined to be the set of pixels with coordinates

$$\{(x-1,y),(x+1,y),(x,y+1),(x,y-1)\} \tag{2}$$

The set of 8-neighbors is the union of the 4-neighbors set with the set of pixels that have the following coordinates

$$\{(x-1,y-1),(x+1,y-1),(x+1,y+1),(x+1,y+1)\} \tag{3}$$

Figure 1 shows examples of 4-neighbor and 8-neighbor pixels.

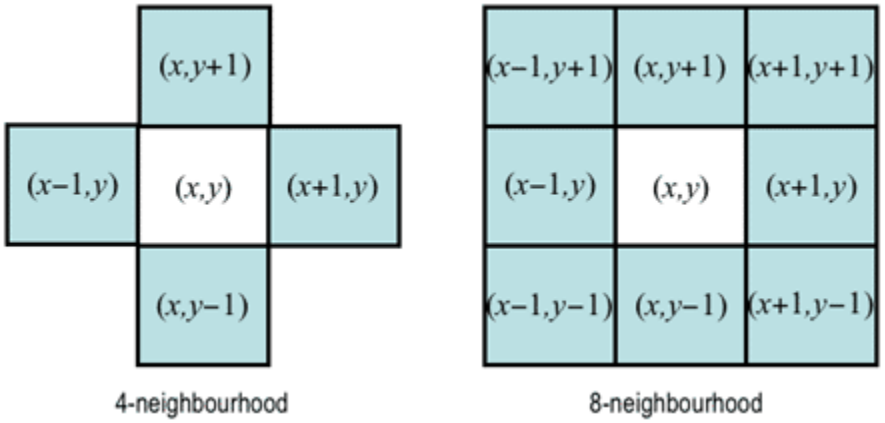

Figure 1: 4-Neighbor and 8-Neighbor Sets

2.1.3 Digital Path

A digital path from pixel p with coordinates (x, y) to pixel q with coordinates (s, t) is a sequence of distinct pixels with coordinates

$$[(x_0, y_0), (x_1, y_1), \dots, (x_n, y_n)] \tag{4}$$

where $(x_0, y_0) = (x, y), (x_n, y_n) = (s, t)$ and the pixels (x_i, y_i) and (x_{i-1}, y_{i-1}) are neighbors for $1 \leq i \leq 0$.

2.1.4 Connectivity

Given an image subset *S*, the pixel *p* and pixel *q* are connected in *S* if there is a path from *p* to *q* that consists entirely of pixels in *S*. For any pixel *p* in *S*, the set of all pixels connected to it in *S* are called a connected component of *S*. If there is only one connected component in *S*, then it is a connected set [1].

2.1.5 Region

A subset of pixels is a region if it is contiguous with uniform grey-level. That is, the pixels form a connected set and the variance in grey-levels among the pixels is small. If two regions R_i and R_j are adjacent, their union forms a connected set. Regions that are not adjacent are considered disjoint [2,3].

2.1.6 Contour

The contour or boundary of a region is the set of pixels that belong to the region such that, for every pixel in the set, at least one of its neighbors is outside the region. One way of representing the discrete objects contained in an image is by the set of pixels that make up their contours.

2.1.7 Descriptor

A descriptor is a feature or set of features used to describe an object. Generally, the features are characteristics that can be quantified as a set of numbers (i.e. vectors in R^d). These numbers are the elements of the descriptor's feature vector. Comparing feature vectors provides an alternative to directly comparing objects [14]. In object recognition, an effective descriptor is one that is invariant to scaling, translation, and rotation of the image.

2.1.8 Segmentation

Segmentation is the process of partitioning an image into disjoint connected sets of pixels. Every image pixel is assigned membership to a set based on specific features of the pixels such as its grey-level. Each set represents a region or object within the image. Segmentation methods typically rely on one of two characteristics: discontinuity or similarity. Generally, discontinuity refers to a significant difference in the intensity in grey-level between pixels. In general,

similarity refers to low variance in grey-level. Two commonly used methods for segmentation are image thresholding and clustering.

2.1.8.1 Image Thresholding

In image thresholding, pixels with a grey-level above a specific value are considered pixels of interest and assigned a value of 1. All other pixels are considered background pixels and assigned a value of 0. The result is a binary image. Methods for determining the threshold value can be classified into two groups: global thresholding and local thresholding. Global thresholding chooses one value that is applied to the entire image. Analysis of the shape of the image histogram is used to determine the specific threshold value. Local thresholding considers the neighbors of each pixel to determine the threshold for that specific value.

2.1.8.2 Clustering-based Segmentation

Clustering refers to a collection of techniques for grouping together patterns of data points into clusters based on a predefined similarity measure. In clustering-based segmentation, pixels are grouped together into regions where each of the pixels in the region are similar with respect to a certain characteristic such as color, texture, or intensity.

One example of clustering algorithms is the *K*-means algorithm. It takes the input parameter, *k*, and partitions a set of *n* objects into *k* clusters so the resulting intra-cluster similarity is high but the inter-cluster similarity is low. Cluster similarity is measured in regard to the mean value of the objects in a cluster, which can be viewed as the cluster's centroid [15]. Within the context of image processing, the algorithm is as follows

1. Pick *k* cluster centers, either randomly or based on some heuristic

2. Assign each pixel in the image to the cluster that minimizes the Euclidean distance between the pixel and the cluster center

3. Re-compute the cluster centers

4. Repeat steps 2 and 3 until no more changes occur or a maximum number of iterations is exceeded.

2.1.9 Connected Component Labeling

Connected Component Labeling (CCL) involves grouping image pixels into subsets of connected pixels. The goal of CCL is to find all the connected components of an image and mark each with a distinctive label.

2.2 Histogram

A frequency distribution is a function showing the number of times a variable takes on a value for each possible value. A frequency histogram is a graphical representation of a frequency distribution. The histogram is constructed by first dividing or binning the range of variables into intervals. A rectangle is placed over each interval with a height equal to the number of times a variable takes on a value that falls within that interval. For example, given a finite set of *n* data points $[z_{1,}\ z_2, \cdots, z_n]$ where each z_i represents an independent measurement, it is possible to define an interval $L = [a, b]$ such that

$$a < min\ z_i\ < \max\ z_i\ < b \tag{5}$$

The interval *L* can then be divided into *m* number of disjoint sub-intervals, or "bins", each of width

$$w = (b - a)/m \tag{6}$$

The interval of each j^{th} bin is therefore defined as

$$B_j = (a + (j - 1)w, a + jw] \tag{7}$$

If n_j is equal to the number of measurements that fall in bin B_j, the result is a frequency distribution. A frequency histogram is constructed by subdividing the horizontal axis of measurement into bins of width *w*, and placing a rectangle over

each j^{th} bin with a height equal to n_j. Figure 2 shows an example of frequency histogram.

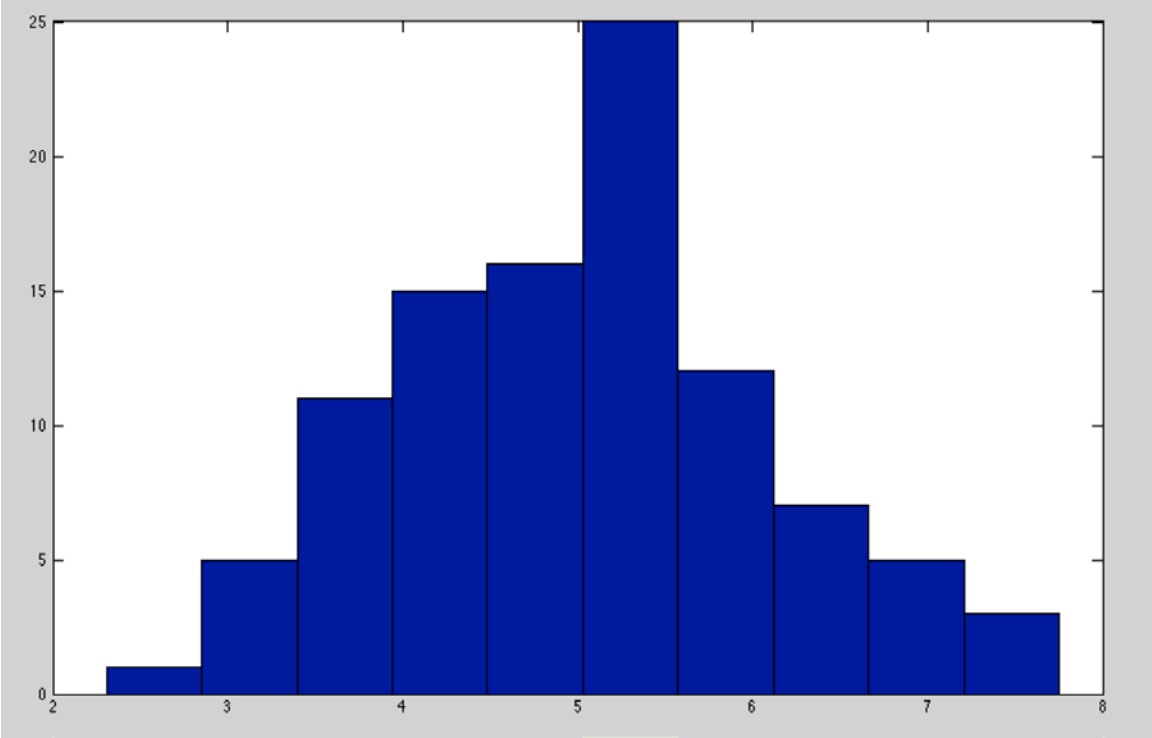

Figure 2: Example Frequency Histogram

The percentage of total measurements in each bin is shown by replacing n_j with $p_j = n_j/n$. The result is a relative frequency histogram that shows the percentage of total measurements in each bin. A relative frequency histogram differs from a frequency histogram only in that the rectangle over each j^{th} bin must have a height equal to p_j.

The probability density function (PDF) is a function that gives the probability that a particular measurement has a certain value. A discrete random variable is a variable that can assume only finite (or countably infinite) number of values [8]. Using those two concepts, the relative frequency histogram can be used to estimate the PDF for a set of measurements. If the center value for the j^{th} bin is defined as follows

$$v_j = (B_{j+1} - B_j)/2 \tag{8}$$

then the center values of the bins can be considered to be a discrete random variable. It is then possible to define the probability for each bin as follows

$$p(v_j) = n_j/n = p_j \tag{9}$$

and therefore the sum of probabilities is equal to one

$$\sum_j p_j = 1 \tag{10}$$

2.3 Object Signature

An object signature represents the object by a one-dimensional function derived from object boundary points. A set of distances from a reference point to the boundary pixels is generated. The reference point is generally the object centroid and the distance can be measured at equal angles, or using every pixel in the boundary. In addition to other requirements, the equal angle methods require the object to be convex; otherwise the same angle may yield more than one distance to the boundary. Using every pixel generates a variable number of samples, which depends on the object. Figure 3 shows the object signature of a circle and square respectively using the equal angle method.

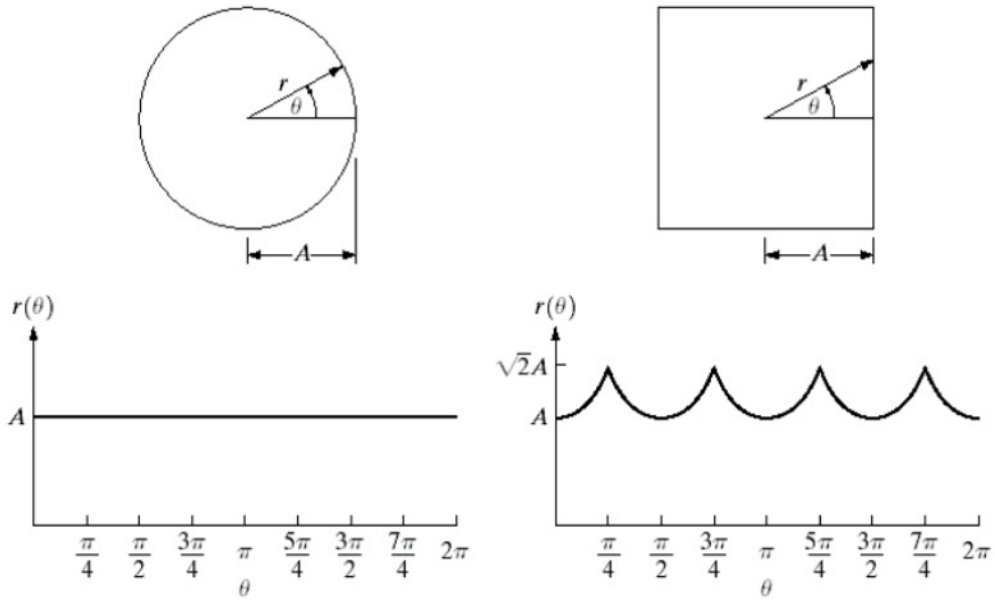

Figure 3: Equal Angle Object Signatures for Circle and Square

2.3.1 Acquiring the Object Signature

In order to obtain an object signature from an image, the image must first be segmented, objects have to be identified, and the pixels that reside on the object boundary have to be marked. Image segmentation can be implemented in several different ways. Following segmentation, connected component labeling and contour following algorithms are applied to identify the boundary pixels and construct the object signature [2, 3].

2.4 Moments

In statistics, moments are a meaningful, numerical description of the distribution of random variables. In physics, they are used to measure the mass distribution of a body. Both interpretations are widely used to describe the geometric shapes of different objects.

2.4.1 Geometric Moments

Given a two-dimensional, continuous image $f(x, y)$, the geometric moment of order $(p + q)$ is defined as

$$m_{pq} = \int_{-\infty}^{+\infty} \int_{-\infty}^{+\infty} x^p y^q f(x, y)\ dx\, dy \tag{11}$$

for $p, q = 0, 1, 2, \ldots$.

The $zero^{th}$ order moment

$$m_{00} = \int_{-\infty}^{+\infty} \int_{-\infty}^{+\infty} f(x, y)\ dx\, dy \tag{12}$$

represents the total mass of the image. In the case of a segmented object, the $zero^{th}$ moment of the object is the total object area [10].

The central moments are defined as

$$\mu_{pq} = \int_{-\infty}^{+\infty} \int_{-\infty}^{+\infty} (x - \overline{x})^p (y - \overline{y})^q f(x, y) \; dx \, dy \tag{13}$$

where

$$\overline{x} = \frac{m_{10}}{m_{00}} \, , \overline{y} = \frac{m_{01}}{m_{00}} \tag{14}$$

After scaling equation (13) by a factor α, the central moments are expressed as

$$\begin{aligned} \mu'_{pq} &= \int_{-\infty}^{+\infty} \int_{-\infty}^{+\infty} (x' - \overline{x}')^p (y' - \overline{y}')^q f'(x', y') \, dx' \, dy' = \\ &= \int_{-\infty}^{+\infty} \int_{-\infty}^{+\infty} \alpha^p (x - \overline{x})^p \alpha^q (y - \overline{y})^q f(x, y) \alpha^2 \, dx \, dy \\ &= \alpha^{p+q+2} \mu_{pq} \end{aligned} \tag{15}$$

Therefore, scale invariance is achieved by normalizing each moment as follows

$$\eta_{pq} = \frac{\mu_{pq}}{{\mu_{00}}^{\gamma}} \tag{16}$$

where

$$\gamma = \frac{p + q}{2} + 1 \tag{17}$$

If $f(x, y)$ is a digital image, the integrals are replaced with summations

$$m_{pq} = \sum_x \sum_y x^p y^q f(x, y) \tag{18}$$

The central moments are expressed as

$$\mu_{pq} = \sum_x \sum_y (x - \bar{x})^p (y - \bar{y})^q f(x, y) \tag{19}$$

2.4.1.1 Hu's Moment Invariants

Developed by Hu in 1962 [7], the following set of moments is invariant to rotation, translation and scaling

$$\phi_1 = \eta_{20} + \eta_{02} \tag{20}$$

$$\phi_2 = (\eta_{20} - \eta_{02})^2 + 4\eta_{11}^2 \tag{21}$$

$$\phi_3 = (\eta_{30} - 3\eta_{12})^2 + (3\eta_{21} - \eta_{03})^2 \tag{22}$$

$$\phi_4 = (\eta_{30} + \eta_{12})^2 + (\eta_{21} + \eta_{03})^2 \tag{23}$$

$$\begin{aligned} \phi_5 = {} & (\eta_{30} - 3\eta_{12})(\eta_{30} + \eta_{12})[(\eta_{30} + \eta_{12})^2 - 3(\eta_{21} + \eta_{03})^2] \\ & + (3\eta_{21} - \eta_{03})(\eta_{21} + \eta_{03})[3(\eta_{30} + \eta_{12})^2 \\ & - (\eta_{21} + \eta_{03})^2] \end{aligned} \tag{24}$$

$$\phi_6 = (\eta_{20} - \eta_{02})[(\eta_{30} + \eta_{12})^2 - (\eta_{21} + \eta_{03})^2] + 4\eta_{11}(\eta_{30} + \eta_{12})(\eta_{21} + \eta_{03}) \quad (25)$$

$$\phi_7 = (3\eta_{21} - \eta_{03})(\eta_{30} + \eta_{12})[(\eta_{30} + \eta_{12})^2 - 3(\eta_{21} + \eta_{03})^2] + (3\eta_{12} - \eta_{30})(\eta_{21} + \eta_{03})[3(\eta_{30} + \eta_{12})^2 - (\eta_{21} + \eta_{03})^2] \quad (26)$$

2.4.2 Contour Moments

Chen shows it is possible to modify the moment equation for two dimensions using the shape contour only

$$m_{pq} = \int_C x^p y^q \, ds \quad (27)$$

where $\int$ is a line integral along the curve C and $ds = \sqrt{((dx)^2 + (dy)^2)}$. The modified central moments are thus defined as

$$\mu_{pq} = \int_C (x - \overline{x})^p (y - \overline{y})^q \, ds, \quad (28)$$

where

$$\overline{x} = \frac{m_{10}}{m_{00}}, \qquad \overline{y} = \frac{m_{01}}{m_{00}} \quad (29)$$

After scaling equation (28) by a factor α, the central moments are expressed as

$$\mu'_{pq} = \int_C \left(x' - \overline{x}'\right)^p \left(y' - \overline{y}'\right)^q \, ds' = \int_C \alpha^p (x - \overline{x})^p \alpha^q (y - \overline{y})^q \, \alpha \, ds = \alpha^{p+q+1} \mu_{pq} \tag{30}$$

Therefore, scale invariance is achieved by normalizing each moment as follows

$$\eta_{pq} = \frac{\mu_{pq}}{{\mu_{00}}^{\gamma}} \tag{31}$$

where

$$\gamma = p + q + 1 \tag{32}$$

For a digital image, the equation becomes

$$\mu_{pq} = \sum_{(x,y) \in C} (x - \overline{x})^p (y - \overline{y})^q \tag{33}$$

The very same functions developed by Hu are then used by Chen to calculate rotation, scaling, and translation invariant moments for the object contour [12,13].

2.4.3 Raw Moments of the Object Signature

It is possible to define the raw, or one-dimensional, moments for an object signature $z = [z_1, z_2, \cdots, z_n]$. The k^{th} moment about the origin is expressed as

$$\mu_k = \frac{1}{n}\sum_i (z_i)^k \tag{34}$$

The first moment or *mean* is defined as

$$m = \frac{1}{n}\sum_i z_i \tag{35}$$

Then the k^{th} moment about the mean is defined as

$$\mu_k = \frac{1}{n}\sum_i (z_i - m)^k \tag{36}$$

The k^{th} normalized moments are expressed as

$$\overline{m}_k = \frac{m_k}{(\mu_2)^{k/2}} \tag{37}$$

$$\overline{\mu}_k = \frac{\mu_k}{(\mu_2)^{k/2}} \tag{38}$$

For an object signature, Gupta and Srinath show the normalized moments (37) and (38) are invariant to rotation, scaling, and translation [4]. They note the coordinates of a transformed shape $H(u, v)$ are related to the original shape $G(x, y)$ by a transformation of the form

$$H(u, v) = A\, G(x, y) + B \tag{39}$$

and provide the following proof [4]. The transformed coordinate variables are given by

$$\begin{bmatrix} u_i \\ v_i \end{bmatrix} = \begin{bmatrix} \alpha \cos\theta & \sin\theta \\ -\sin\theta & \alpha \cos\theta \end{bmatrix} \begin{bmatrix} x_i \\ y_i \end{bmatrix} + \begin{bmatrix} \beta \\ \gamma \end{bmatrix} \tag{40}$$

where β and γ are the translation variables, α is the scale factor, and θ is the angle through which the shape is rotated.

Let the contour of the original shape be G and that of the transformed shape be H

$$G = [g(1), g(2), \ldots, g(N)] \tag{41}$$

$$H = [h(1), h(2), \ldots, h(M)] \tag{42}$$

where

$$g(l) = [(x_l - \overline{x})^2 + (y_l - \overline{y})^2]^{1/2} \tag{43}$$

$$h(k) = [(u_k - \overline{u})^2 + (v_k - \overline{v})^2]^{1/2} \tag{44}$$

$(\overline{x}, \overline{y})$ is the centroid of the original shape and it is given as

$$\overline{x} = \frac{m_{10}}{m_{00}}, \qquad \overline{y} = \frac{m_{01}}{m_{00}} \tag{45}$$

where

$$m_{pq} = \sum_x \sum_y x^p y^q \, G(x, y) \tag{46}$$

is the $(p+q)^{th}$ geometric moment of the shape function $G(x, y)$. Similarly, $(\overline{u}, \overline{v})$ is the centroid of the transformed shape. Let ${m_k}^H$ represent the k^{th} moment of $H(u, v)$. From equations (37) and (38), the normalized contour moments of shape $H(u, v)$ are

$$\overline{m}_k{}^H = \frac{\frac{1}{M}\sum_k [h(k)]^k}{\left[\frac{1}{M}\sum_k [h(k) - {m_1}^H]^2\right]^{k/2}} \tag{47}$$

$$\overline{M}_k{}^H = \frac{\frac{1}{M}\sum_k [h(k) - {m_1}^H]^k}{\left[\frac{1}{M}\sum_k [h(k) - {m_1}^H]^2\right]^{k/2}} \tag{48}$$

By substituting (40) in (44) and using the resulting $h(k)$ in (47) and (48), the normalized moments $\overline{m}_k{}^H$ and $\overline{M}_k{}^H$ of the transformed shape $H(u, v)$ are expressed

in terms of the original coordinate variables (x, y). Using the definitions of normalized moments given in equations (37) and (38), and some algebraic manipulations, it can be shown that

$$\overline{m}_k{}^H = \overline{m}_k{}^G \tag{49}$$

$$\overline{M}_k{}^H = \overline{M}_k{}^G \tag{50}$$

Gupta and Srinath then define the following set of descriptors that are invariant to shape translation, rotation and scaling

$$F_1 = \frac{(\mu_2)^{1/2}}{m} \tag{51}$$

$$F_2 = \frac{\mu_3}{(\mu_2)^{3/2}} \tag{52}$$

$$F_3 = \frac{\mu_4}{(\mu_2)^2} \tag{53}$$

$$F_4 = \frac{\mu_5}{(\mu_2)^{5/2}} \tag{54}$$

2.4.4 Moments of a Random Variable

Let $y = [y_1, y_2, \cdots, y_m]$ be the set of all possible distances from a boundary pixel to the centroid in the object signature. Let Y be a discrete random variable for the number of times a distance value occurs in the set y. The probability $p(\mathrm{Y} = y_i)$ of distance y_i occurring in a given signature is calculated as

$$p(y_i) = \frac{n_i}{n} \tag{55}$$

where n_i is the number of times that the distance y_i occurs in the signature and *n* is the total number of elements in *y*. Their sum must be equal to one

$$\sum_i p(y_i) = 1 \tag{56}$$

with the mean given as

$$m = \sum_i y_i \, p(y_i) \tag{57}$$

The k^{th} moment about the mean is then defined as

$$\mu_k = \sum_i (y_i - m)^k \, p(y_i) \tag{58}$$

2.4.4.1 Normalized Moments of a Random Variable

To compensate for changes in scale, it is necessary to normalize the moments. For any change in scale α, the set y becomes

$$\alpha\, y = [\alpha\, y_1, \alpha\, y_2, \cdots, \alpha\, y_m] \tag{59}$$

The mean is then defined as

$$m' = \sum_i \alpha\, y_i\, p(y_i) = \alpha \sum_i y_i\, p(y_i) = \alpha\, m \tag{60}$$

and the k^{th}moment about the mean becomes

$$\begin{aligned} \mu_k' &= \sum_i (\alpha\, y_i - \alpha\, m)^k\, p(y_i) = \sum_i \alpha^k\, (y_i - m)^k\, p(y_i) \\ &= \alpha^k \sum_i (y_i - m)^k\, p(y_i) = \alpha^k\, \mu_k \end{aligned} \tag{61}$$

The normalized k^{th}moment about the mean can therefore be calculated as

$$\overline{m}_k = \frac{\alpha^k\, \mu_k}{(\alpha\, m)^k} = \frac{\mu_k}{m^k} \tag{62}$$

2.4.5 Histogram Moments

It is possible to approximate the raw moments of the object signature using the relative frequency histogram of the set $y = [y_1, y_2, \cdots, y_m]$. The center bin-values of the histogram are considered to be a discrete random variable and the relative frequencies are considered the PDF. To be more precise, let the set *v* contain the center bin-values. The approximation follows

$$m \approx m' = \sum_j v_j p_j \tag{63}$$

where v_j is the value assigned to the j^{th} bin and p_j is the relative frequency for that bin. The k^{th} moment about the mean is approximated as

$$\mu_k \approx \mu'_k = \sum_j (v_j - m')^k p_j \tag{64}$$

2.4.5.1. Histogram Moment Descriptors

The following set of descriptors is proposed to leverage the use of moments of the histogram

$$F_1 = \frac{\mu_2}{m^2} \tag{65}$$

$$F_2 = \frac{\mu_3}{m^3} \tag{66}$$

$$F_3 = \frac{\mu_4}{m^4} \tag{67}$$

The second, third, and fourth moments of the histogram of the object signature are each divided by the first moment raised to the second, third, and fourth power respectively. This ensures the descriptors are invariant to scaling. Since the object signature is never zero in our experiments, the mean is always non-zero and hence division by zero is not a concern. These descriptors only require the use of four moments of the histogram compared to the five raw moments used by Gupta and Srinath's set of four descriptors.

2.5 Fourier Descriptors

The Fourier Descriptor is a technique used for representing shapes. They are simple to compute, intuitive, and easy to normalize. In addition, they are robust to noise and capture both global and local features [5]. The descriptors represent the shape of the object in a frequency domain and avoid the high cost of matching shape signatures in the spatial domain [6]. The Discrete Fourier

Transform is applied to a function of the contour coordinates to obtain the Fourier Descriptor. Figure 4 shows a *K*-point digital boundary in the *xy*-plane.

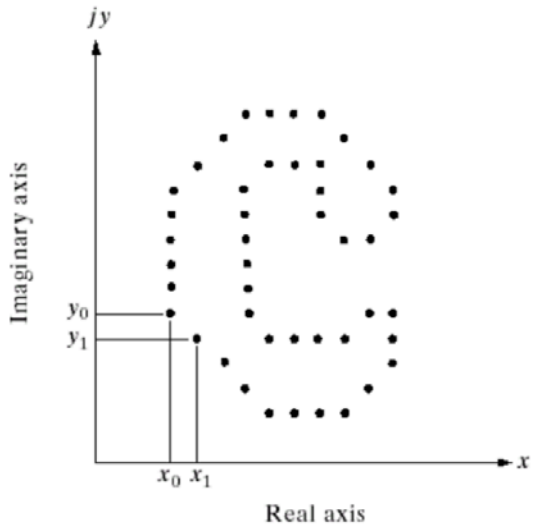

Figure 4: K-Point Digital Boundary in the xy-plane

The coordinate pairs $(x_0, y_0), (x_1, y_1), (x_2, y_2) \dots, (x_{k-1}, y_{k-1})$ can be expressed in the form $x(k) = x_k$ and $y(k) = y_k$. The boundary can be represented as a sequence of coordinates $s(k) = [x(k), y(k)]$, for $k = 0,1,2 \dots, k-1$. Each coordinate pair is expressed as a complex number

$$s(k) = x(k) + jy(k) \tag{68}$$

The *x*-axis is treated as the real axis and the *y*-axis is treated as the imaginary axis. The Discrete Fourier Transform of $s(k)$ is

$$a_n = \sum_k s(k) e^{-j2\pi k/K} \tag{69}$$

for $n = 0,1,2 \ldots, K-1$ [1]. The coefficients a_n are referred to as the Fourier Descriptors. The one-dimensional Discrete Fourier Transform of an object signature can be calculated as

$$a_n = \frac{1}{N} \sum_t z(t) e^{-j2\pi nu/N} \tag{70}$$

Where *z(t)* is the object signature for $n = 0,1,2 \ldots, N-1$. Hu and Li explain that rotation invariance of the Fourier Descriptors is achieved by ignoring the phase information, only taking into consideration the magnitude values [6]. Scale invariance for real-valued signatures is established by dividing the magnitude of the first half descriptors by the DC components $|a_0|$. Since $|a_0|$ is always the largest coefficient, the values of the normalized descriptors should be in the range from zero to one [6]

$$V = \left|\frac{a_1}{a_0}\right|, \left|\frac{a_2}{a_0}\right|, \left|\frac{a_3}{a_0}\right|, \ldots, \left|\frac{a_{N/2}}{a_0}\right| \tag{71}$$

2.6 Mean Square Error

The Mean Square Error (MSE) is an average of the squared errors. In this thesis we define error to be a distance between corresponding elements of two descriptor feature vectors representing image objects. It is computed as follows

$$MSE = \frac{1}{n}\sum_{k}\left[F_k^i - F_k^r\right]^2 \;\; k = 1..n \tag{72}$$

where F_k^i is the k^{th} element of the n element vector representing object *i* and F_k^r is the k^{th} element of the n element vector representing object *r*.

2.7 Confusion Matrix

Results of experiments are presented in this paper using a confusion matrix. A confusion matrix is a matrix where element $\left[m_{i,j}\right]$ of the matrix *m* is the Mean Square Error (MSE) between the element assigned to row *i* and the element assigned to column *j*. For each row in the matrix, the column with the lowest MSE is considered a match. An MSE of zero is an exact match while a higher MSE is indicative of dissimilarity between the two elements. An error occurs when $\left[m_{i,j}\right]$ is a match but the element assigned to row *i* is not the same as the element assigned to row *j*.

2.8 Star-Convex

A set of points is considered convex if for any two points in the set, all points on the line segment connecting the two points are included in the set. A set is considered to be star-convex if there exists at least one point such that for any other point in the set, all points on the line segment connecting the two points are included in the set.

III. RELATED WORK

In this section, relevant research is discussed and compared to the method presented in this paper. This thesis presents a novel method for recognizing objects in images. The method utilizes a minimum number of moments of the histogram of the object signature, and requires far less computation operations, resulting in effective, accurate descriptors. Previous research has applied moments to the entire image or directly to the contour or the object signature. This is the first work that investigates applying moments to the histogram of the object signature.

Hu presented the first significant research into the use of moments for two-dimensional image analysis and recognition [7]. Based on the method of algebraic invariants, Hu derived a set of seven moments using nonlinear combinations of lower order regular moments. This set of moments is invariant to translation, scaling, and rotation but is a region-based method that treats shapes as a whole. The moments must be computed over all pixels of an object, including the contour. This is in stark contrast to the method introduced in this work, which utilizes moments of the histogram of the object signature. When calculating the moments of the histogram of the object signature, only the center bin-values of the constructed histogram are used. As a result, the savings in computation are

significant and provide computational complexity that is orders of magnitude smaller than using every pixel of the image. In addition, the descriptors introduced in this thesis only require computing four moments as opposed to seven, and only pixels in the object contour are required.

Chen proposed a modified version of Hu's method involving the same moment invariants, requiring computation over just the pixels that make up the object contour [12]. However, like Hu, Chen's method requires computing seven moments as opposed to the method introduced in this thesis which only requires four. Although Chen's method is computationally less costly than Hu's, it uses every pixel in the contour and therefore, in general, it is expected to be less efficient than using the histogram of the object signature.

Mandal et al. offer an approach that employs statistical moments of a random variable [15]. They suggest treating the intensity values of image pixels as a random variable and using the normalized image histogram as an approximation of the PDF for pixel intensities. Moments of the random variable are then calculated and used to describe the object. This is a region-based approach that requires consideration of all pixels in the object, including the contour. Our method utilizing moments of the histogram of the object signature only involve pixels that make up the contour of the object and since only the

center bin-values of the histogram are used to calculate moments, the savings in computation are substantial.

Gonzales and Woods suggest representing a segment of the boundary for an object as a one-dimensional function of an arbitrary variable [1]. The amplitude of the function is treated as a discrete random variable and a normalized frequency histogram is used to estimate the PDF for the random variable. Moments of the random variable are then calculated and used to describe the shape. However, the authors do not use the entire contour of the object nor do they use the object signature.

Gupta and Srinath use the moments of a signature derived from the contour pixels of an object to generate descriptors that are invariant to translation, rotation, and scaling [4]. The paper, however, requires the contour pixels to be organized into an ordered sequence before computing the Euclidean distance between contour pixels and the object centroid to produce the signature. In addition, the authors do not group the signature values into a histogram before calculating the moments. Consequently, they use every element of the object signature to calculate each moment in contrast to the method introduced in this paper, which only uses the center value of each bin in the histogram. In general, far less computation is necessary. Furthermore, Gupta and Srinath require five moments to derive their descriptors. The method introduced in this work only requires four.

IV. EXPERIMENTAL SETUP

This section discusses the setup of the experiments and how results are presented and evaluated. The goal of the experiments is to compare the effectiveness of various descriptors in recognizing objects that have been translated, scaled, and rotated. The descriptors evaluated in these experiments are as follows:

1. Moment Invariants
2. Moment Invariants of the Object Contour
3. 2D Fourier Descriptors of the Object Contour
4. Moments of the Object Signature
5. Moments of the Histogram of the Object Signature
6. 1D Fourier Descriptors of the Object Signature

4.1 Software

The experiments for this thesis were developed and implemented using the MATLAB computing environment (version 7.14.0.739).

4.2 Hardware

A 2.8 GHz Intel Core i5 processor running 64-bit Mac OS X version 10.9.5 was used to run the experiments.

4.3 Dataset

A library of synthetic images is constructed. Each image is a binary image made up of a background and one set of pixels representing a simple, filled-in object. Ten base objects are considered: five basic geometric shapes and five random star-convex objects. Each object is scaled, rotated, and then scaled and rotated to produce 40 different objects in total. The five basic geometric shapes are circle, ellipse, square, rectangle, and arrow. Figure 5 through Figure 9 show the five basic geometric shapes:

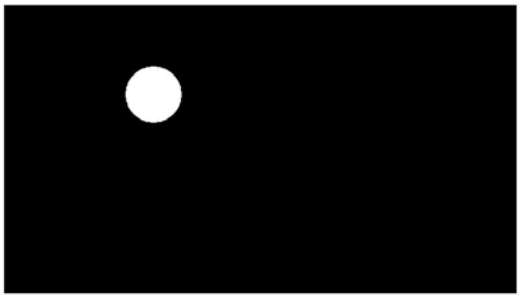

Figure 5: Circle

Figure 6: Ellipse

Figure 7: Square

Figure 8: Rectangle

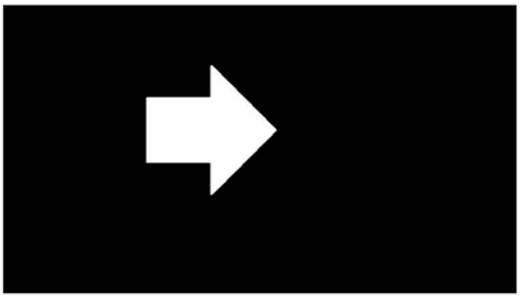

Figure 9: Arrow

The five star-convex objects were created using eight, sixteen, twenty-nine, thirty-seven, and forty-five randomly generated vertices. Figure 10 through figure 14 show the five non-convex, star-convex objects.

Figure 10: 8 Point Star-Convex

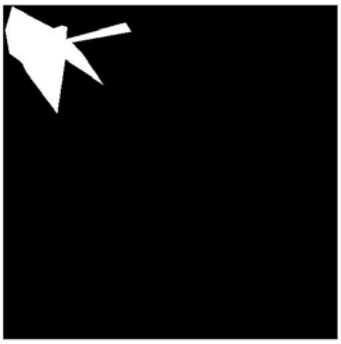

Figure 11: 16 Point Star-Convex

Figure 12: 29 Point Star-Convex

Figure 13: 37 Point Star-Convex

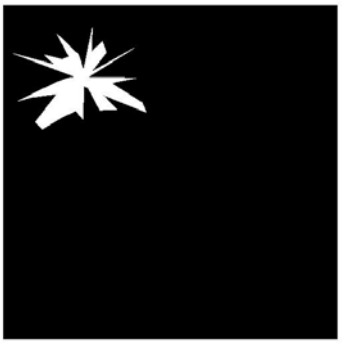

Figure 14: 45 Point Star-Convex

4.4 Descriptors

The descriptors, listed above, are grouped into two classes: region-based (which use all the pixels in the shape) and contour-based (which use information involving the boundary pixels only). The region-based descriptor class consists of Hu's set of seven moment invariants. The class of contour-based descriptors

includes moments of the object signature, moments of the histogram of the object signature, two-dimensional Fourier descriptors of the object contour, one-dimensional Fourier descriptors of the object signature, and Chen's application of Hu's moment invariants to the object contour. The object signature is obtained by calculating the Euclidean distance from the centroid of the object to each pixel in the object contour.

4.5 Process

In each experiment, a different descriptor is used to compare the objects in the library against the objects in a database made up of the ten base objects. First, the descriptor feature vectors are computed for all objects in the library and database. Then a confusion matrix is constructed where each row is assigned the feature vector representing an input object O_l from the library and each column is assigned a feature vector representing a reference object O_d from the database. The result is a 40 x 10 matrix. Each element $[m_{i,r}]$ of the matrix is the Mean Square Error (MSE) between the feature vector assigned to row *i* and the feature vector assigned to column *r*. For each row, the column with the smallest MSE is considered a match. An MSE of zero is an exact match while a higher MSE is indicative of dissimilarity. If the feature vectors representing two objects are a match, then the objects they represent are considered to be a match. An error occurs when an input object O_l from the library is a match with a reference object O_d from the database but the two objects are not the same. For example, if the

scaled and rotated arrow object from the library is identified as a match with the square object from the database, the result is considered an error.

4.6 Comparison

Descriptors are compared using recognition accuracy in addition to the quality of recognition in the experiment. An effective descriptor should have an MSE close to zero for matches and a relatively large MSE for non-matches. For these experiments, the Quality Recognition score is computed by taking the ratio of average MSE for matches, $\overline{M}_m$, to average MSE for non-matches, $\overline{M}_n$

$$q = \frac{\overline{M}_m}{\overline{M}_n}$$

The quality of recognition improves as the q number approaches zero.

The Recognition Rate is the ratio of correct matches to total possible correct matches

$$r = \frac{M - E}{M}$$

where, E is the total number of errors and M is the total number of possible correct matches. For each of the experiments in this thesis, $M = 40$.

V. EXPERIMENTS AND RESULTS

In this section, the experiments conducted as part of this thesis are discussed. Six experiments in total are performed. For each experiment, a confusion matrix that displays the recognition accuracy is presented. The results of each experiment are compared using recognition accuracy. Quality of recognition is used to contrast only those methods that achieve a 100% recognition rate. In the resulting confusion matrices, matches are highlighted in yellow for each experiment. An experiment with 100% recognition shows all matches along the diagonal. Matches that are off the diagonal are incorrect and count against the recognition rate.

Experiment 1

The first experiment evaluates Hu's set of seven moment-invariant descriptors as shown in equations (20) – (26). Table 1 shows the confusion matrix derived in the experiment.

	Arrow	Ellipse	Circle	Random 8	Random 16	Random 29	Random 37	Random 45	Rectangle	Square
Arrow	0	0.00296203	7.92E-05	0.0011394	0.00071067	0.00075816	0.00091311	0.00090896	0.00043722	3.71E-05
Rotated Arrow	7.62E-32	0.00296203	7.92E-05	0.0011394	0.00071067	0.00075816	0.00091311	0.00090896	0.00043722	3.71E-05
Scaled Arrow	1.16E-12	0.00296193	7.92E-05	0.00113933	0.00071061	0.0007581	0.00091304	0.0009089	0.00043718	3.71E-05
Scaled Rotated Arrow	1.16E-12	0.00296193	7.92E-05	0.00113933	0.00071061	0.0007581	0.00091304	0.0009089	0.00043718	3.71E-05
Ellipse	0.00296203	0	0.00394646	0.00045016	0.00113734	0.00091947	0.00096677	0.00090966	0.00112632	0.00363171
Rotated Ellipse	0.00296203	4.37E-35	0.00394646	0.00045016	0.00113734	0.00091947	0.00096677	0.00090966	0.00112632	0.00363171
Scaled Ellipse	0.00296254	2.77E-11	0.00394706	0.00045034	0.00113757	0.00091969	0.00096696	0.00090985	0.00112663	0.00363228
Scaled Rotated Ellipse	0.00296254	2.77E-11	0.00394706	0.00045034	0.00113757	0.00091969	0.00096696	0.00090985	0.00112663	0.00363228
Circle	7.92E-05	0.00394646	0	0.0017989	0.00125485	0.00132633	0.00152523	0.00152182	0.00087058	8.05E-06
Rotated Circle	7.92E-05	0.00394646	2.16E-32	0.0017989	0.00125485	0.00132633	0.00152523	0.00152182	0.00087058	8.05E-06
Scaled Circle	7.91E-05	0.00394602	1.44E-11	0.0017986	0.00125459	0.00132605	0.00152493	0.00152153	0.00087037	8.03E-06
Scaled Rotated Circle	7.91E-05	0.00394602	1.44E-11	0.0017986	0.00125459	0.00132605	0.00152493	0.00152153	0.00087037	8.03E-06
Random 8	0.0011394	0.00045016	0.0017989	0	0.00018979	9.87E-05	0.00015639	0.0001272	0.00016812	0.00157939
Rotated Random 8	0.0011394	0.00045016	0.0017989	5.03E-33	0.00018979	9.87E-05	0.00015639	0.0001272	0.00016812	0.00157939
Scaled Random 8	0.00114144	0.00044897	0.00180147	9.17E-10	0.00019029	9.91E-05	0.00015669	0.00012749	0.0001689	0.00158179
Scaled Rotated Random 8	0.00114144	0.00044897	0.00180147	9.17E-10	0.00019029	9.91E-05	0.00015669	0.00012749	0.0001689	0.00158179
Random 16	0.00071067	0.00113734	0.00125485	0.00018979	0	1.92E-05	2.09E-05	2.06E-05	0.0001488	0.00106355
Rotated Random 16	0.00071067	0.00113734	0.00125485	0.00018979	4.67E-30	1.92E-05	2.09E-05	2.06E-05	0.0001488	0.00106355
Scaled Random 16	0.0007047	0.00114192	0.00124694	0.00019074	1.26E-08	1.93E-05	2.17E-05	2.14E-05	0.00014699	0.00105627
Scaled Rotated Random 16	0.0007047	0.00114192	0.00124694	0.00019074	1.26E-08	1.93E-05	2.17E-05	2.14E-05	0.00014699	0.00105627
Random 29	0.00075816	0.00091947	0.00132633	9.87E-05	1.92E-05	0	1.99E-05	1.24E-05	1.00E-04	0.0011297
Rotated Random 29	0.00075816	0.00091947	0.00132633	9.87E-05	1.92E-05	3.48E-33	1.99E-05	1.24E-05	1.00E-04	0.0011297
Scaled Random 29	0.00076634	0.00091406	0.00133713	9.79E-05	1.93E-05	2.34E-08	1.89E-05	1.15E-05	0.00010274	0.00113965
Scaled Rotated Random 29	0.00076634	0.00091406	0.00133713	9.79E-05	1.93E-05	2.34E-08	1.89E-05	1.15E-05	0.00010274	0.00113965
Random 37	0.00091311	0.00096677	0.00152523	0.00015639	2.09E-05	1.99E-05	0	1.66E-06	0.00020415	0.00131205
Rotated Random 37	0.00091311	0.00096677	0.00152523	0.00015639	2.09E-05	1.99E-05	2.34E-32	1.66E-06	0.00020415	0.00131205
Scaled Random 37	0.00091342	0.00096659	0.00152563	0.00015638	2.10E-05	1.99E-05	2.60E-11	1.66E-06	0.00020426	0.00131242
Scaled Rotated Random 37	0.00091342	0.00096659	0.00152563	0.00015638	2.10E-05	1.99E-05	2.60E-11	1.66E-06	0.00020426	0.00131242
Random 45	0.00090896	0.00090966	0.00152182	0.0001272	2.06E-05	1.24E-05	1.66E-06	0	0.00018223	0.00130932
Rotated Random 45	0.00090896	0.00090966	0.00152182	0.0001272	2.06E-05	1.24E-05	1.66E-06	3.97E-32	0.00018223	0.00130932
Scaled Random 45	0.00092073	0.00090125	0.00153705	0.00012605	2.21E-05	1.34E-05	1.75E-06	3.86E-08	0.00018613	0.00132346
Scaled Rotated Random 45	0.00092073	0.00090125	0.00153705	0.00012605	2.21E-05	1.34E-05	1.75E-06	3.86E-08	0.00018613	0.00132346
Rectangle	0.00043722	0.00112632	0.00087058	0.00016812	0.0001488	1.00E-04	0.00020415	0.00018223	0	0.00072101
Rotated Rectangle	0.00043722	0.00112632	0.00087058	0.00016812	0.0001488	1.00E-04	0.00020415	0.00018223	0	0.00072101
Scaled Rectangle	0.00043728	0.00112624	0.00087066	0.00016808	0.00014878	9.99E-05	0.00020412	0.0001822	1.98E-12	0.00072108
Scaled Rotated Rectangle	0.00043728	0.00112624	0.00087066	0.00016808	0.00014878	9.99E-05	0.00020412	0.0001822	1.98E-12	0.00072108
Square	3.71E-05	0.00363171	8.05E-06	0.00157939	0.00106355	0.0011297	0.00131205	0.00130932	0.00072101	0
Rotated Square	3.71E-05	0.00363171	8.05E-06	0.00157939	0.00106355	0.0011297	0.00131205	0.00130932	0.00072101	0
Scaled Square	3.71E-05	0.00363158	8.06E-06	0.0015793	0.00106348	0.00112962	0.00131197	0.00130923	0.00072095	1.37E-12
Scaled Rotated Square	3.71E-05	0.00363158	8.06E-06	0.0015793	0.00106348	0.00112962	0.00131197	0.00130923	0.00072095	1.37E-12

Table 1: Experiment 1 Results

Table 1 shows a 100% Recognition Rate. The Quality Recognition Score is .000044842.

Experiment 2

The second experiment evaluates Chen's application of Hu's moments to the object contour. The results are shown in Table 2.

	Arrow	Ellipse	Circle	Random 8	Random 16	Random 29	Random 37	Random 45	Rectangle	Square
Arrow	0	2.91E-06	2.07E-05	3.34E-06	1.11E-05	2.76E-05	3.73E-05	3.81E-05	5.02E-07	4.99E-07
Rotated Arrow	6.19E-35	2.91E-06	2.07E-05	3.34E-06	1.11E-05	2.76E-05	3.73E-05	3.81E-05	5.02E-07	4.99E-07
Scaled Arrow	3.19E-06	1.22E-05	4.02E-05	1.30E-05	2.40E-06	1.20E-05	1.87E-05	1.92E-05	6.21E-06	6.21E-06
Scaled Rotated Arrow	3.19E-06	1.22E-05	4.02E-05	1.30E-05	2.40E-06	1.20E-05	1.87E-05	1.92E-05	6.21E-06	6.21E-06
Ellipse	2.91E-06	0	8.15E-06	1.65E-08	2.54E-05	4.83E-05	6.09E-05	6.20E-05	9.94E-07	1.00E-06
Rotated Ellipse	2.91E-06	3.87E-34	8.15E-06	1.65E-08	2.54E-05	4.83E-05	6.09E-05	6.20E-05	9.94E-07	1.00E-06
Scaled Ellipse	2.01E-07	1.60E-06	1.70E-05	1.93E-06	1.42E-05	3.24E-05	4.28E-05	4.37E-05	7.34E-08	8.07E-08
Scaled Rotated Ellipse	2.01E-07	1.60E-06	1.70E-05	1.93E-06	1.42E-05	3.24E-05	4.28E-05	4.37E-05	7.34E-08	8.07E-08
Circle	2.07E-05	8.15E-06	0	7.45E-06	6.22E-05	9.61E-05	0.00011361	0.00011503	1.48E-05	1.48E-05
Rotated Circle	2.07E-05	8.15E-06	3.96E-33	7.45E-06	6.22E-05	9.61E-05	0.00011361	0.00011503	1.48E-05	1.48E-05
Scaled Circle	7.97E-07	6.69E-07	1.34E-05	8.80E-07	1.79E-05	3.77E-05	4.90E-05	4.99E-05	3.77E-08	3.46E-08
Scaled Rotated Circle	7.97E-07	6.69E-07	1.34E-05	8.80E-07	1.79E-05	3.77E-05	4.90E-05	4.99E-05	3.77E-08	3.46E-08
Random 8	3.34E-06	1.65E-08	7.45E-06	0	2.66E-05	5.01E-05	6.29E-05	6.40E-05	1.26E-06	1.26E-06
Rotated Random 8	3.34E-06	1.65E-08	7.45E-06	6.88E-36	2.66E-05	5.01E-05	6.29E-05	6.40E-05	1.26E-06	1.26E-06
Scaled Random 8	3.12E-06	4.97E-09	7.79E-06	3.78E-09	2.60E-05	4.92E-05	6.19E-05	6.30E-05	1.12E-06	1.13E-06
Scaled Rotated Random 8	3.12E-06	4.97E-09	7.79E-06	3.78E-09	2.60E-05	4.92E-05	6.19E-05	6.30E-05	1.12E-06	1.13E-06
Random 16	1.11E-05	2.54E-05	6.22E-05	2.66E-05	0	3.67E-06	7.68E-06	8.05E-06	1.63E-05	1.63E-05
Rotated Random 16	1.11E-05	2.54E-05	6.22E-05	2.66E-05	1.72E-36	3.67E-06	7.68E-06	8.05E-06	1.63E-05	1.63E-05
Scaled Random 16	1.11E-05	2.54E-05	6.22E-05	2.66E-05	4.44E-13	3.67E-06	7.68E-06	8.05E-06	1.63E-05	1.63E-05
Scaled Rotated Random 16	1.11E-05	2.54E-05	6.22E-05	2.66E-05	4.44E-13	3.67E-06	7.68E-06	8.05E-06	1.63E-05	1.63E-05
Random 29	2.76E-05	4.83E-05	9.61E-05	5.01E-05	3.67E-06	0	7.31E-07	8.49E-07	3.55E-05	3.55E-05
Rotated Random 29	2.76E-05	4.83E-05	9.61E-05	5.01E-05	3.67E-06	1.66E-46	7.31E-07	8.49E-07	3.55E-05	3.55E-05
Scaled Random 29	2.80E-05	4.89E-05	9.70E-05	5.07E-05	3.84E-06	1.94E-09	6.57E-07	7.70E-07	3.60E-05	3.60E-05
Scaled Rotated Random 29	2.80E-05	4.89E-05	9.70E-05	5.07E-05	3.84E-06	1.94E-09	6.57E-07	7.70E-07	3.60E-05	3.60E-05
Random 37	3.73E-05	6.09E-05	0.00011361	6.29E-05	7.68E-06	7.31E-07	0	4.45E-09	4.64E-05	4.64E-05
Rotated Random 37	3.73E-05	6.09E-05	0.00011361	6.29E-05	7.68E-06	7.31E-07	2.42E-37	4.45E-09	4.64E-05	4.64E-05
Scaled Random 37	4.15E-05	6.63E-05	0.00012091	6.84E-05	9.66E-06	1.42E-06	1.14E-07	7.31E-08	5.11E-05	5.11E-05
Scaled Rotated Random 37	4.15E-05	6.63E-05	0.00012091	6.84E-05	9.66E-06	1.42E-06	1.14E-07	7.31E-08	5.11E-05	5.11E-05
Random 45	3.81E-05	6.20E-05	0.00011503	6.40E-05	8.05E-06	8.49E-07	4.45E-09	0	4.73E-05	4.73E-05
Rotated Random 45	3.81E-05	6.20E-05	0.00011503	6.40E-05	8.05E-06	8.49E-07	4.45E-09	3.62E-43	4.73E-05	4.73E-05
Scaled Random 45	3.84E-05	6.24E-05	0.00011555	6.44E-05	8.19E-06	8.94E-07	8.25E-09	5.83E-10	4.76E-05	4.76E-05
Scaled Rotated Random 45	3.84E-05	6.24E-05	0.00011555	6.44E-05	8.19E-06	8.94E-07	8.25E-09	5.83E-10	4.76E-05	4.76E-05
Rectangle	5.02E-07	9.94E-07	1.48E-05	1.26E-06	1.63E-05	3.55E-05	4.64E-05	4.73E-05	0	3.02E-09
Rotated Rectangle	5.02E-07	9.94E-07	1.48E-05	1.26E-06	1.63E-05	3.55E-05	4.64E-05	4.73E-05	0	3.02E-09
Scaled Rectangle	5.02E-07	9.94E-07	1.48E-05	1.26E-06	1.63E-05	3.55E-05	4.64E-05	4.73E-05	6.45E-14	2.99E-09
Scaled Rotated Rectangle	5.02E-07	9.94E-07	1.48E-05	1.26E-06	1.63E-05	3.55E-05	4.64E-05	4.73E-05	6.45E-14	2.99E-09
Square	4.99E-07	1.00E-06	1.48E-05	1.26E-06	1.63E-05	3.55E-05	4.64E-05	4.73E-05	3.02E-09	0
Rotated Square	4.99E-07	1.00E-06	1.48E-05	1.26E-06	1.63E-05	3.55E-05	4.64E-05	4.73E-05	3.02E-09	0
Scaled Square	4.99E-07	1.00E-06	1.48E-05	1.26E-06	1.63E-05	3.55E-05	4.64E-05	4.73E-05	3.02E-09	5.47E-15
Scaled Rotated Square	4.99E-07	1.00E-06	1.48E-05	1.26E-06	1.63E-05	3.55E-05	4.64E-05	4.73E-05	3.02E-09	5.47E-15

Table 2: Experiment 2 Results

The experiment incorrectly identifies the scaled arrow and the scaled and rotated arrow as the star-convex object with 16 vertices, the scaled ellipse and the scaled and rotated ellipse are identified as the rectangle, and it identifies the scaled circle and the scaled and rotated circle as the square. The eight incorrect matches result in a Recognition Rate of 80%.

Experiment 3

The third experiment evaluates two-dimensional Fourier descriptors of the object contour. The results are shown in Table 3.

	Arrow	Ellipse	Circle	Random 8	Random 16	Random 29	Random 37	Random 45	Rectangle	Square
Arrow	0	2.22E-04	8.86E-05	1.94E-03	1.95E-03	9.38E-04	7.68E-04	5.61E-04	6.14E-04	1.52E-04
Rotated Arrow	3.66E-07	2.21E-04	7.84E-05	1.96E-03	1.98E-03	9.53E-04	7.74E-04	5.69E-04	6.19E-04	1.40E-04
Scaled Arrow	7.72E-05	3.12E-04	2.41E-04	1.76E-03	1.41E-03	7.71E-04	5.11E-04	4.25E-04	5.94E-04	2.01E-04
Scaled Rotated Arrow	7.32E-05	3.08E-04	2.30E-04	1.78E-03	1.43E-03	7.80E-04	5.14E-04	4.30E-04	5.96E-04	1.91E-04
Ellipse	2.22E-04	0	2.14E-04	1.19E-03	2.12E-03	9.63E-04	7.26E-04	4.88E-04	1.39E-04	2.61E-04
Rotated Ellipse	1.96E-04	1.21E-06	1.83E-04	1.25E-03	2.13E-03	9.68E-04	7.28E-04	4.92E-04	1.65E-04	2.31E-04
Scaled Ellipse	5.65E-04	1.03E-04	6.12E-04	6.82E-04	2.05E-03	1.01E-03	8.31E-04	5.59E-04	2.23E-05	6.54E-04
Scaled Rotated Ellipse	5.56E-04	9.90E-05	6.04E-04	6.87E-04	2.05E-03	1.01E-03	8.26E-04	5.55E-04	2.23E-05	6.45E-04
Circle	8.86E-05	2.14E-04	0	2.29E-03	2.59E-03	1.26E-03	0.00095114	0.00075427	6.73E-04	5.86E-05
Rotated Circle	8.90E-05	2.13E-04	2.65E-09	2.29E-03	2.59E-03	1.26E-03	0.00095081	0.00075406	6.72E-04	5.84E-05
Scaled Circle	8.91E-05	2.15E-04	2.79E-07	2.30E-03	2.61E-03	1.27E-03	9.67E-04	7.61E-04	6.79E-04	6.67E-05
Scaled Rotated Circle	8.93E-05	2.16E-04	2.82E-07	2.30E-03	2.62E-03	1.27E-03	9.68E-04	7.62E-04	6.80E-04	6.67E-05
Random 8	1.94E-03	1.19E-03	2.29E-03	0	1.45E-03	1.24E-03	1.49E-03	1.16E-03	6.41E-04	2.25E-03
Rotated Random 8	2.37E-03	1.53E-03	2.76E-03	2.27E-05	1.58E-03	1.49E-03	1.78E-03	1.44E-03	8.80E-04	2.71E-03
Scaled Random 8	1.96E-03	1.21E-03	2.31E-03	1.10E-07	1.45E-03	1.26E-03	1.51E-03	1.18E-03	6.54E-04	2.28E-03
Scaled Rotated Random 8	2.04E-03	1.27E-03	2.39E-03	1.34E-06	1.47E-03	1.30E-03	1.55E-03	1.22E-03	6.91E-04	2.35E-03
Random 16	1.95E-03	2.12E-03	2.59E-03	1.45E-03	0	1.13E-03	1.35E-03	1.40E-03	1.85E-03	2.30E-03
Rotated Random 16	7.03E-05	2.10E-04	1.71E-04	1.58E-03	1.43E-03	7.30E-04	5.65E-04	4.27E-04	4.86E-04	1.45E-04
Scaled Random 16	1.93E-03	2.11E-03	2.56E-03	1.49E-03	1.16E-06	1.14E-03	1.32E-03	1.40E-03	1.85E-03	2.26E-03
Scaled Rotated Random 16	5.03E-04	6.61E-04	8.23E-04	1.21E-03	4.92E-04	5.63E-04	5.37E-04	4.91E-04	7.16E-04	6.83E-04
Random 29	9.38E-04	9.63E-04	1.26E-03	1.24E-03	1.13E-03	0	5.66E-04	2.37E-04	9.54E-04	1.27E-03
Rotated Random 29	1.01E-03	1.03E-03	1.34E-03	1.26E-03	1.12E-03	1.34E-06	5.94E-04	2.63E-04	1.01E-03	1.35E-03
Scaled Random 29	9.77E-04	1.00E-03	1.31E-03	1.25E-03	1.09E-03	2.14E-06	5.76E-04	2.48E-04	9.76E-04	1.31E-03
Scaled Rotated Random 29	8.04E-04	8.38E-04	1.10E-03	1.24E-03	1.12E-03	6.47E-06	5.09E-04	1.92E-04	8.54E-04	1.11E-03
Random 37	7.68E-04	7.26E-04	0.00095114	1.49E-03	1.35E-03	5.66E-04	0	2.01E-04	6.88E-04	7.56E-04
Rotated Random 37	5.68E-04	5.49E-04	0.00071379	1.49E-03	1.41E-03	5.47E-04	1.71E-05	1.63E-04	5.80E-04	5.53E-04
Scaled Random 37	7.53E-04	7.30E-04	0.00094324	1.53E-03	1.35E-03	5.98E-04	3.51E-06	2.23E-04	7.01E-04	7.45E-04
Scaled Rotated Random 37	5.56E-04	5.53E-04	0.00070896	1.52E-03	1.41E-03	5.76E-04	2.07E-05	1.84E-04	5.90E-04	5.46E-04
Random 45	5.61E-04	4.88E-04	0.00075427	1.16E-03	1.40E-03	2.37E-04	2.01E-04	0	5.05E-04	7.18E-04
Rotated Random 45	3.69E-04	3.32E-04	0.00051304	1.25E-03	1.50E-03	3.08E-04	2.25E-04	2.32E-05	4.27E-04	4.93E-04
Scaled Random 45	9.41E-04	8.28E-04	0.00121278	1.14E-03	1.33E-03	2.23E-04	2.62E-04	5.54E-05	7.33E-04	1.15E-03
Scaled Rotated Random 45	5.89E-04	5.23E-04	0.00079271	1.17E-03	1.38E-03	2.34E-04	2.09E-04	1.59E-06	5.35E-04	7.55E-04
Rectangle	6.14E-04	1.39E-04	6.73E-04	6.41E-04	1.85E-03	9.54E-04	6.88E-04	5.05E-04	0	6.58E-04
Rotated Rectangle	6.60E-04	1.63E-04	7.25E-04	6.05E-04	1.85E-03	9.69E-04	7.04E-04	5.21E-04	9.61E-07	7.06E-04
Scaled Rectangle	8.22E-04	2.52E-04	9.04E-04	5.06E-04	1.86E-03	1.03E-03	7.69E-04	5.90E-04	1.70E-05	8.75E-04
Scaled Rotated Rectangle	8.10E-04	2.44E-04	8.90E-04	5.13E-04	1.86E-03	1.03E-03	7.64E-04	5.85E-04	1.51E-05	8.62E-04
Square	1.52E-04	2.61E-04	5.86E-05	2.25E-03	2.30E-03	1.27E-03	7.56E-04	7.18E-04	6.58E-04	0
Rotated Square	1.55E-04	2.63E-04	6.16E-05	2.25E-03	2.30E-03	1.27E-03	7.52E-04	7.19E-04	6.59E-04	3.84E-08
Scaled Square	1.90E-04	2.96E-04	9.46E-05	2.27E-03	2.25E-03	1.30E-03	7.26E-04	7.33E-04	6.77E-04	4.31E-06
Scaled Rotated Square	1.85E-04	2.91E-04	8.93E-05	2.27E-03	2.26E-03	1.30E-03	7.30E-04	7.31E-04	6.75E-04	3.24E-06

Table 3: Experiment 3 Results

The scaled ellipse and the scaled and rotated ellipse are incorrectly identified as the rectangle, the rotated star-convex object with 16 vertices was incorrectly identified as the arrow, and the scaled and rotated star-convex object

with 16 vertices is misidentified as the star-convex object with 45 vertices. The resulting Recognition Rate is 90%.

Experiment 4

The fourth experiment evaluates the four descriptors derived by Gupta and Srinath in equations (53) – (56) applied to the object signature. The results are shown in Table 4.

	Arrow	Ellipse	Circle	Random 8	Random 16	Random 29	Random 37	Random 45	Rectangle	Square
Arrow	0	2.61E+00	1.25E+00	4.57E+00	1.01E+01	1.38E-01	9.42E-01	2.58E+00	5.60E-01	5.22E+00
Rotated Arrow	1.66E-05	2.60E+00	1.24E+00	4.55E+00	1.01E+01	1.35E-01	9.34E-01	2.57E+00	5.54E-01	5.20E+00
Scaled Arrow	1.13E-01	3.77E+00	2.10E+00	5.97E+00	1.21E+01	4.03E-01	1.60E+00	3.68E+00	1.17E+00	6.77E+00
Scaled Rotated Arrow	1.08E-01	3.74E+00	2.08E+00	5.94E+00	1.21E+01	3.95E-01	1.59E+00	3.65E+00	1.16E+00	6.73E+00
Ellipse	2.61E+00	0	3.03E-01	4.33E-01	2.75E+00	1.79E+00	5.65E-01	7.66E-02	8.88E-01	5.10E-01
Rotated Ellipse	2.52E+00	8.71E-04	2.73E-01	4.67E-01	2.85E+00	1.72E+00	5.31E-01	7.97E-02	8.33E-01	5.52E-01
Scaled Ellipse	1.93E+00	5.67E-02	1.12E-01	7.66E-01	3.58E+00	1.27E+00	3.45E-01	1.54E-01	4.96E-01	8.98E-01
Scaled Rotated Ellipse	1.89E+00	6.28E-02	1.05E-01	7.86E-01	3.62E+00	1.24E+00	3.36E-01	1.61E-01	4.79E-01	9.21E-01
Circle	1.25E+00	3.03E-01	0	1.31E+00	4.69E+00	7.98E-01	0.23026653	0.40824735	2.02E-01	1.47E+00
Rotated Circle	1.36E+00	2.49E-01	2.99E-03	1.19E+00	4.46E+00	8.75E-01	0.23936013	0.34987828	2.51E-01	1.34E+00
Scaled Circle	1.30E+00	2.78E-01	4.42E-02	1.07E+00	4.29E+00	7.54E-01	1.16E-01	2.73E-01	3.23E-01	1.32E+00
Scaled Rotated Circle	1.17E+00	3.36E-01	4.10E-02	1.20E+00	4.54E+00	6.60E-01	9.79E-02	3.34E-01	2.70E-01	1.46E+00
Random 8	4.57E+00	4.33E-01	1.31E+00	0	1.09E+00	3.31E+00	1.39E+00	2.91E-01	2.40E+00	1.04E-01
Rotated Random 8	5.31E+00	6.30E-01	1.68E+00	2.81E-02	7.79E-01	3.95E+00	1.81E+00	4.92E-01	2.90E+00	7.61E-02
Scaled Random 8	4.83E+00	4.92E-01	1.43E+00	3.77E-03	9.76E-01	3.53E+00	1.54E+00	3.55E-01	2.56E+00	8.41E-02
Scaled Rotated Random 8	5.18E+00	5.87E-01	1.60E+00	1.97E-02	8.30E-01	3.84E+00	1.74E+00	4.53E-01	2.80E+00	7.32E-02
Random 16	1.01E+01	2.75E+00	4.69E+00	1.09E+00	0	8.17E+00	4.92E+00	2.51E+00	6.66E+00	9.62E-01
Rotated Random 16	1.10E+01	3.24E+00	5.32E+00	1.41E+00	2.00E-02	8.98E+00	5.56E+00	2.97E+00	7.41E+00	1.25E+00
Scaled Random 16	9.63E+00	2.51E+00	4.37E+00	9.41E-01	5.67E-03	7.75E+00	4.60E+00	2.27E+00	6.28E+00	8.25E-01
Scaled Rotated Random 16	1.01E+01	2.73E+00	4.67E+00	1.08E+00	6.63E-05	8.13E+00	4.89E+00	2.49E+00	6.63E+00	9.53E-01
Random 29	1.38E-01	1.79E+00	7.98E-01	3.31E+00	8.17E+00	0	4.10E-01	1.68E+00	3.78E-01	3.95E+00
Rotated Random 29	6.94E-02	2.26E+00	1.10E+00	3.95E+00	9.15E+00	2.87E-02	6.54E-01	2.15E+00	5.45E-01	4.65E+00
Scaled Random 29	1.55E-01	1.71E+00	7.52E-01	3.21E+00	8.01E+00	8.23E-04	3.75E-01	1.61E+00	3.55E-01	3.84E+00
Scaled Rotated Random 29	1.11E-01	1.93E+00	8.86E-01	3.50E+00	8.47E+00	2.75E-03	4.79E-01	1.82E+00	4.24E-01	4.16E+00
Random 37	9.42E-01	5.65E-01	0.23026653	1.39E+00	4.92E+00	4.10E-01	0	4.40E-01	3.41E-01	1.85E+00
Rotated Random 37	8.57E-01	6.38E-01	0.25435279	1.51E+00	5.13E+00	3.51E-01	2.43E-03	5.07E-01	3.27E-01	1.98E+00
Scaled Random 37	8.67E-01	6.31E-01	0.2518947	1.49E+00	5.11E+00	3.57E-01	1.99E-03	5.00E-01	3.31E-01	1.97E+00
Scaled Rotated Random 37	8.22E-01	6.74E-01	0.2675543	1.56E+00	5.23E+00	3.27E-01	5.17E-03	5.40E-01	3.25E-01	2.04E+00
Random 45	2.58E+00	7.66E-02	0.40824735	2.91E-01	2.51E+00	1.68E+00	4.40E-01	0	1.03E+00	5.06E-01
Rotated Random 45	2.81E+00	8.23E-02	0.48666036	2.21E-01	2.29E+00	1.87E+00	5.37E-01	5.01E-03	1.17E+00	4.16E-01
Scaled Random 45	2.50E+00	7.01E-02	0.37376468	3.22E-01	2.60E+00	1.62E+00	4.09E-01	8.50E-04	9.75E-01	5.39E-01
Scaled Rotated Random 45	2.61E+00	6.97E-02	0.40941149	2.84E-01	2.49E+00	1.71E+00	4.54E-01	2.51E-04	1.04E+00	4.91E-01
Rectangle	5.60E-01	8.88E-01	2.02E-01	2.40E+00	6.66E+00	3.78E-01	3.41E-01	1.03E+00	0	2.69E+00
Rotated Rectangle	5.60E-01	8.88E-01	2.02E-01	2.40E+00	6.66E+00	3.78E-01	3.41E-01	1.03E+00	8.76E-09	2.69E+00
Scaled Rectangle	5.63E-01	8.84E-01	2.00E-01	2.39E+00	6.65E+00	3.80E-01	3.41E-01	1.03E+00	4.93E-06	2.69E+00
Scaled Rotated Rectangle	5.62E-01	8.86E-01	2.01E-01	2.39E+00	6.66E+00	3.79E-01	3.41E-01	1.03E+00	1.97E-06	2.69E+00
Square	5.22E+00	5.10E-01	1.47E+00	1.04E-01	9.62E-01	3.95E+00	1.85E+00	5.06E-01	2.69E+00	0
Rotated Square	5.22E+00	5.10E-01	1.47E+00	1.04E-01	9.62E-01	3.95E+00	1.85E+00	5.06E-01	2.69E+00	0.00E+00
Scaled Square	5.25E+00	5.20E-01	1.49E+00	1.08E-01	9.51E-01	3.98E+00	1.87E+00	5.17E-01	2.72E+00	6.16E-05
Scaled Rotated Square	5.25E+00	5.20E-01	1.49E+00	1.08E-01	9.51E-01	3.98E+00	1.87E+00	5.17E-01	2.72E+00	6.18E-05

Table 4: Experiment 4 Results

The experiment correctly identifies all objects with zero errors, therefore the resulting Recognition Rate is 100%. The Quality Recognition Score is calculated to be 0.0673.

Experiment 5

The fifth experiment evaluates the application of moments to the histogram of the object signature. For this experiment the new set of descriptors introduced in equations (65) – (67) are used. The results are shown in Table 5.

	Arrow	Ellipse	Circle	Random 8	Random 16	Random 29	Random 37	Random 45	Rectangle	Square
Arrow	0	4.11E-03	3.64E-04	3.78E-03	2.63E-03	2.87E-03	2.83E-03	5.66E-03	6.65E-04	1.75E-04
Rotated Arrow	7.95E-10	4.11E-03	3.65E-04	3.78E-03	2.63E-03	2.87E-03	2.83E-03	5.66E-03	6.64E-04	1.76E-04
Scaled Arrow	3.93E-06	4.36E-03	2.93E-04	4.01E-03	2.81E-03	3.08E-03	3.04E-03	5.94E-03	7.71E-04	1.27E-04
Scaled Rotated Arrow	3.90E-06	4.36E-03	2.93E-04	4.01E-03	2.81E-03	3.08E-03	3.03E-03	5.94E-03	7.71E-04	1.27E-04
Ellipse	4.11E-03	0	6.78E-03	7.54E-05	3.59E-04	3.83E-04	2.35E-04	2.14E-04	1.60E-03	5.86E-03
Rotated Ellipse	4.05E-03	4.63E-07	6.71E-03	7.88E-05	3.58E-04	3.60E-04	2.18E-04	2.24E-04	1.55E-03	5.79E-03
Scaled Ellipse	3.46E-03	4.59E-05	5.98E-03	1.38E-04	3.48E-04	2.00E-04	1.04E-04	3.76E-04	1.16E-03	5.11E-03
Scaled Rotated Ellipse	3.44E-03	5.00E-05	5.95E-03	1.43E-04	3.51E-04	1.93E-04	9.96E-05	3.84E-04	1.14E-03	5.08E-03
Circle	3.64E-04	6.78E-03	0	6.24E-03	4.64E-03	5.17E-03	0.0051064	0.00864924	2.01E-03	3.58E-05
Rotated Circle	3.64E-04	6.78E-03	9.15E-13	6.24E-03	4.64E-03	5.17E-03	0.00510627	0.00864908	2.01E-03	3.58E-05
Scaled Circle	3.68E-04	6.79E-03	8.24E-09	6.25E-03	4.65E-03	5.18E-03	5.12E-03	8.66E-03	2.02E-03	3.69E-05
Scaled Rotated Circle	3.68E-04	6.79E-03	8.36E-09	6.25E-03	4.65E-03	5.18E-03	5.12E-03	8.67E-03	2.02E-03	3.69E-05
Random 8	3.78E-03	7.54E-05	6.24E-03	0	1.73E-04	4.38E-04	2.41E-04	2.49E-04	1.52E-03	5.38E-03
Rotated Random 8	3.80E-03	9.29E-05	6.25E-03	4.26E-06	1.50E-04	5.17E-04	2.96E-04	2.83E-04	1.56E-03	5.39E-03
Scaled Random 8	3.71E-03	8.10E-05	6.14E-03	1.02E-06	1.50E-04	4.52E-04	2.48E-04	2.78E-04	1.48E-03	5.29E-03
Scaled Rotated Random 8	3.72E-03	8.89E-05	6.14E-03	3.40E-06	1.40E-04	4.89E-04	2.74E-04	2.95E-04	1.50E-03	5.30E-03
Random 16	2.63E-03	3.59E-04	4.64E-03	1.73E-04	0	6.46E-04	3.90E-04	8.35E-04	9.94E-04	3.91E-03
Rotated Random 16	2.72E-03	3.78E-04	4.73E-03	1.77E-04	1.93E-06	7.04E-04	4.34E-04	8.38E-04	1.07E-03	4.00E-03
Scaled Random 16	2.49E-03	3.72E-04	4.46E-03	1.93E-04	2.54E-06	6.07E-04	3.64E-04	8.78E-04	8.97E-04	3.75E-03
Scaled Rotated Random 16	2.52E-03	3.80E-04	4.50E-03	1.94E-04	1.21E-06	6.33E-04	3.83E-04	8.80E-04	9.29E-04	3.78E-03
Random 29	2.87E-03	3.83E-04	5.17E-03	4.38E-04	6.46E-04	0	3.44E-05	6.86E-04	8.60E-04	4.39E-03
Rotated Random 29	2.97E-03	4.33E-04	5.28E-03	4.99E-04	7.39E-04	3.46E-06	5.77E-05	7.10E-04	9.20E-04	4.50E-03
Scaled Random 29	2.85E-03	3.74E-04	5.14E-03	4.25E-04	6.24E-04	2.04E-07	3.01E-05	6.84E-04	8.45E-04	4.36E-03
Scaled Rotated Random 29	2.89E-03	3.94E-04	5.19E-03	4.51E-04	6.66E-04	1.99E-07	3.92E-05	6.92E-04	8.73E-04	4.42E-03
Random 37	2.83E-03	2.35E-04	0.0051064	2.41E-04	3.90E-04	3.44E-05	0	5.48E-04	8.42E-04	4.33E-03
Rotated Random 37	2.82E-03	2.47E-04	0.00509182	2.53E-04	4.04E-04	2.98E-05	2.07E-07	5.59E-04	8.37E-04	4.32E-03
Scaled Random 37	2.46E-03	3.17E-04	0.00460363	3.07E-04	3.67E-04	4.72E-05	1.37E-05	7.23E-04	6.42E-04	3.86E-03
Scaled Rotated Random 37	2.44E-03	3.25E-04	0.00458812	3.15E-04	3.75E-04	4.55E-05	1.46E-05	7.32E-04	6.37E-04	3.85E-03
Random 45	5.66E-03	2.14E-04	0.00864924	2.49E-04	8.35E-04	6.86E-04	5.48E-04	0	2.66E-03	7.64E-03
Rotated Random 45	5.74E-03	2.24E-04	0.00874405	2.50E-04	8.33E-04	7.44E-04	5.91E-04	1.89E-06	2.73E-03	7.73E-03
Scaled Random 45	5.58E-03	1.97E-04	0.00856159	2.38E-04	8.17E-04	6.52E-04	5.19E-04	5.48E-07	2.59E-03	7.56E-03
Scaled Rotated Random 45	5.62E-03	2.00E-04	0.00860289	2.37E-04	8.13E-04	6.79E-04	5.38E-04	2.99E-07	2.63E-03	7.59E-03
Rectangle	6.65E-04	1.60E-03	2.01E-03	1.52E-03	9.94E-04	8.60E-04	8.42E-04	2.66E-03	0	1.52E-03
Rotated Rectangle	6.66E-04	1.60E-03	2.01E-03	1.52E-03	9.93E-04	8.60E-04	8.42E-04	2.66E-03	1.55E-12	1.52E-03
Scaled Rectangle	6.56E-04	1.61E-03	1.99E-03	1.53E-03	1.00E-03	8.71E-04	8.52E-04	2.67E-03	3.50E-08	1.50E-03
Scaled Rotated Rectangle	6.56E-04	1.61E-03	1.99E-03	1.53E-03	1.00E-03	8.71E-04	8.52E-04	2.67E-03	3.68E-08	1.50E-03
Square	1.75E-04	5.86E-03	3.58E-05	5.38E-03	3.91E-03	4.39E-03	4.33E-03	7.64E-03	1.52E-03	0
Rotated Square	1.75E-04	5.86E-03	3.58E-05	5.38E-03	3.91E-03	4.39E-03	4.33E-03	7.64E-03	1.52E-03	0.00E+00
Scaled Square	1.76E-04	5.86E-03	3.54E-05	5.39E-03	3.92E-03	4.40E-03	4.33E-03	7.65E-03	1.52E-03	1.59E-09
Scaled Rotated Square	1.76E-04	5.86E-03	3.54E-05	5.39E-03	3.92E-03	4.40E-03	4.33E-03	7.65E-03	1.52E-03	1.55E-09

Table 5: Experiment 5 Results

The experiment correctly identifies all objects. The resulting Recognition Rate is 100%. The Quality Recognition Score is 0.0128.

Experiment 6

The sixth experiment evaluates one-dimensional Fourier descriptors of the object signature.

	Arrow	Ellipse	Circle	Random 8	Random 16	Random 29	Random 37	Random 45	Rectangle	Square
Arrow	0	2.61E-03	1.26E-03	2.10E-03	1.58E-03	2.46E-03	2.91E-03	3.18E-03	1.22E-03	1.34E-03
Rotated Arrow	5.31E-07	2.58E-03	1.26E-03	2.09E-03	1.57E-03	2.48E-03	2.89E-03	3.15E-03	1.19E-03	1.32E-03
Scaled Arrow	1.18E-04	3.42E-03	1.11E-03	2.53E-03	1.38E-03	2.59E-03	2.82E-03	3.40E-03	1.79E-03	1.16E-03
Scaled Rotated Arrow	1.13E-04	3.40E-03	1.12E-03	2.53E-03	1.40E-03	2.59E-03	2.83E-03	3.42E-03	1.78E-03	1.17E-03
Ellipse	2.61E-03	0	5.26E-03	8.65E-04	4.42E-03	5.89E-03	6.78E-03	5.38E-03	3.92E-04	5.37E-03
Rotated Ellipse	2.61E-03	1.98E-06	5.25E-03	9.28E-04	4.49E-03	5.93E-03	6.82E-03	5.46E-03	3.89E-04	5.37E-03
Scaled Ellipse	2.51E-03	1.81E-05	5.00E-03	9.26E-04	4.60E-03	5.84E-03	6.93E-03	5.58E-03	3.74E-04	5.24E-03
Scaled Rotated Ellipse	2.50E-03	2.22E-05	4.99E-03	9.57E-04	4.63E-03	5.85E-03	6.94E-03	5.61E-03	3.74E-04	5.24E-03
Circle	1.26E-03	5.26E-03	0	4.75E-03	4.03E-03	4.37E-03	0.00431101	0.00549829	2.96E-03	4.04E-04
Rotated Circle	1.26E-03	5.26E-03	1.19E-09	4.75E-03	4.03E-03	4.37E-03	0.0043114	0.00549892	2.96E-03	4.04E-04
Scaled Circle	1.26E-03	5.27E-03	1.90E-06	4.81E-03	4.07E-03	4.39E-03	4.32E-03	5.55E-03	2.95E-03	3.98E-04
Scaled Rotated Circle	1.26E-03	5.27E-03	1.93E-06	4.82E-03	4.07E-03	4.39E-03	4.32E-03	5.55E-03	2.96E-03	3.98E-04
Random 8	2.10E-03	8.65E-04	4.75E-03	0	2.65E-03	4.10E-03	5.91E-03	4.34E-03	1.01E-03	4.97E-03
Rotated Random 8	2.09E-03	8.55E-04	4.74E-03	3.80E-07	2.66E-03	4.13E-03	5.90E-03	4.33E-03	1.00E-03	4.96E-03
Scaled Random 8	2.07E-03	8.22E-04	4.73E-03	8.58E-07	2.65E-03	4.10E-03	5.89E-03	4.35E-03	9.72E-04	4.94E-03
Scaled Rotated Random 8	2.07E-03	8.18E-04	4.72E-03	1.08E-06	2.66E-03	4.11E-03	5.89E-03	4.35E-03	9.68E-04	4.94E-03
Random 16	1.58E-03	4.42E-03	4.03E-03	2.65E-03	0	3.15E-03	2.47E-03	2.80E-03	3.02E-03	2.97E-03
Rotated Random 16	1.62E-03	4.52E-03	4.03E-03	2.66E-03	3.84E-06	3.15E-03	2.51E-03	2.80E-03	3.10E-03	2.99E-03
Scaled Random 16	1.59E-03	4.43E-03	3.97E-03	2.72E-03	5.17E-06	3.29E-03	2.41E-03	2.82E-03	2.99E-03	2.86E-03
Scaled Rotated Random 16	1.61E-03	4.48E-03	3.97E-03	2.72E-03	5.31E-06	3.29E-03	2.43E-03	2.82E-03	3.04E-03	2.87E-03
Random 29	2.46E-03	5.89E-03	4.37E-03	4.10E-03	3.15E-03	0	3.42E-03	2.60E-03	4.46E-03	4.61E-03
Rotated Random 29	2.45E-03	5.78E-03	4.38E-03	3.88E-03	3.06E-03	1.18E-05	3.43E-03	2.50E-03	4.39E-03	4.64E-03
Scaled Random 29	2.42E-03	5.85E-03	4.35E-03	4.02E-03	3.09E-03	5.92E-06	3.43E-03	2.52E-03	4.43E-03	4.61E-03
Scaled Rotated Random 29	2.41E-03	5.79E-03	4.36E-03	3.91E-03	3.06E-03	1.37E-05	3.44E-03	2.48E-03	4.40E-03	4.63E-03
Random 37	2.91E-03	6.78E-03	0.00431101	5.91E-03	2.47E-03	3.42E-03	0	1.52E-03	4.63E-03	3.03E-03
Rotated Random 37	2.86E-03	6.61E-03	0.00427946	5.61E-03	2.31E-03	3.36E-03	1.64E-05	1.39E-03	4.52E-03	3.02E-03
Scaled Random 37	2.76E-03	6.70E-03	0.00409263	5.85E-03	2.48E-03	3.42E-03	2.01E-05	1.54E-03	4.53E-03	2.87E-03
Scaled Rotated Random 37	2.73E-03	6.62E-03	0.00407477	5.71E-03	2.39E-03	3.39E-03	2.65E-05	1.47E-03	4.48E-03	2.86E-03
Random 45	3.18E-03	5.38E-03	0.00549829	4.34E-03	2.80E-03	2.60E-03	1.52E-03	0	4.05E-03	4.70E-03
Rotated Random 45	3.19E-03	5.35E-03	0.00552925	4.34E-03	2.86E-03	2.58E-03	1.55E-03	2.01E-06	4.04E-03	4.74E-03
Scaled Random 45	3.14E-03	5.35E-03	0.00548251	4.37E-03	2.85E-03	2.62E-03	1.58E-03	8.61E-06	4.03E-03	4.71E-03
Scaled Rotated Random 45	3.15E-03	5.33E-03	0.00549768	4.38E-03	2.88E-03	2.60E-03	1.59E-03	1.11E-05	4.02E-03	4.73E-03
Rectangle	1.22E-03	3.92E-04	2.96E-03	1.01E-03	3.02E-03	4.46E-03	4.63E-03	4.05E-03	0	2.90E-03
Rotated Rectangle	1.22E-03	3.92E-04	2.96E-03	1.01E-03	3.02E-03	4.46E-03	4.63E-03	4.05E-03	1.48E-11	2.90E-03
Scaled Rectangle	1.22E-03	3.99E-04	2.95E-03	1.04E-03	3.05E-03	4.47E-03	4.64E-03	4.08E-03	2.73E-07	2.89E-03
Scaled Rotated Rectangle	1.22E-03	3.99E-04	2.95E-03	1.05E-03	3.05E-03	4.47E-03	4.64E-03	4.08E-03	3.28E-07	2.89E-03
Square	1.34E-03	5.37E-03	4.04E-04	4.97E-03	2.97E-03	4.61E-03	3.03E-03	4.70E-03	2.90E-03	0
Rotated Square	1.34E-03	5.37E-03	4.04E-04	4.97E-03	2.97E-03	4.61E-03	3.03E-03	4.70E-03	2.90E-03	0.00E+00
Scaled Square	1.35E-03	5.39E-03	4.05E-04	5.01E-03	3.01E-03	4.63E-03	3.04E-03	4.73E-03	2.91E-03	3.21E-07
Scaled Rotated Square	1.35E-03	5.39E-03	4.05E-04	5.01E-03	3.01E-03	4.63E-03	3.04E-03	4.73E-03	2.91E-03	3.23E-07

Table 6: Experiment 6 Results

The experiment correctly identifies all objects, resulting in a Recognition Rate of 100% with a Quality Recognition Score of 0.0281.

VI. RESULTS EVALUATION

This section evaluates the results of the experiments outlined in the previous chapter. Six experiments in total are performed, each conducted to evaluate the use of specific descriptors to recognize objects in a segmented image. First, the Recognition Rate is compared. Next, the Quality of Recognition is used to differentiate between the methods that achieve a 100% Recognition Rate. Table 7 shows the Recognition Rate of each of the experiments. Four of the experiments correctly identify every object in the library and achieve a 100% Recognition Rate. Those experiments are Hu's set of seven moment-invariant descriptors, Gupta and Srinath's set of four descriptors of the object signature, the set of three descriptors introduced in this work generated from moments of the histogram of the object signature, and one-dimensional Fourier descriptors of the object signature. Chen's application of Hu's moments to the object contour incorrectly identify eight objects and achieves an 80% Recognition Rate. Two-dimensional Fourier descriptors of the object contour incorrectly identify four objects and achieve a 90% recognition rate.

Experiment	Descriptor	Recognition Rate
Experiment 1	Hu's set of seven moment invariants	100%
Experiment 2	Chen's application of Hu's moments to the object contour	80%
Experiment 3	2D Fourier descriptors of the object contour	90%
Experiment 4	Gupta & Srinath descriptors applied to the object signature	100%
Experiment 5	Moments of the histogram of the object signature	100%
Experiment 6	1D Fourier descriptors of the object signature	100%

Table 7: Recognition Rates of Experiments

In order to compare those descriptors that achieve a 100% Recognition Rate, we take into consideration the Quality of Recognition. Table 8 shows the Quality Recognition Score for each experiment. The lower the score, the more accurate the descriptor. Hu's set of seven moment invariants scores the lowest with 4.4842e-05. The next lowest score belongs to our descriptors generated from moments of the histogram of the object signature with a score of 0.0128. One-dimensional Fourier descriptors of the object contour are next with a score of 0.0281. Finally, Gupta and Srinath's four descriptors generate a score of 0.0673.

Experiment	Descriptor	Quality of recognition
Experiment 1	Hu's set of seven moment invariants	4.4842e-05
Experiment 4	Four descriptors derived by Gupta & Srinath applied to the object signature	0.0673
Experiment 5	Moments of the histogram of the object signature	0.0128
Experiment 6	1D Fourier descriptors of the object signature	0.0281

Table 8: Quality Recognition Scores of Experiments

Hu's set of seven moment invariants performed better than all other methods. This is expected since it uses all the pixels of the image and therefore uses more information compared to methods that only consider the object contour. Hu's moment invariants have a superior Quality of Recognition score but they are computationally expensive and higher order moments are hard to derive. It can be seen from equation (11) that the double integrals are to be considered over the whole area of the object including its boundary [19]. Chen's application of Hu's moments only considers the object contour and therefore it reduces the computational complexity. However, this method has the most errors of all the descriptors with eight incorrect matches. Every error involved identifying scaled

objects. Using only the boundary pixels reduces the amount of information to be processed. The method introduced in this work, taking moments of the histogram of the object signature, only uses the center bin-values of the constructed histogram to calculate moments. The computational costs are orders of magnitude smaller than methods that use every pixel of the image or even just pixels of the object contour.

The descriptors based on moments of the histogram of the object signature introduced in this thesis show an improvement over those based on raw moments, such as the methods proposed by Gupta and Srinath. Although both sets of descriptors achieve a 100% Recognition Rate, the descriptors derived in this work achieve a better Quality of Recognition score. The effect of binning the data when constructing the histogram compensates for any noise introduced due to scaling an object. In addition, only four moments are required compared to Gupta and Srinath, who use five. The computational complexity is reduced by the method introduced in this thesis, since the moments are calculated using the bin-values of the histogram of the object signature. The calculations used in deriving Gupta and Srinath's descriptors involve every element of the object signature. The result is a significant improvement in efficiency.

Based on the results of the experiments, the method introduced in this thesis, taking the moments of the histogram of the object signature, proves to be more accurate than all other methods with the exception of Hu's moment invariants.

Although Hu's moment invariants are more accurate, taking moments of the histogram of the object signature is computationally less expensive.

Conclusion

With the explosion of data generated in the form of images and video, there is a growing need to develop methods and techniques to automate their analysis, such as recognizing and matching objects in images. The goal of this thesis is to compare various descriptors that do just that. The six experiments show that the region-based moment invariants developed by Hu performed best. However, it was demonstrated that Fourier Descriptors and descriptors that utilize moments of the object signature are viable alternatives. Among those, the set of descriptors derived in this work based on moments of the histogram of the object signature, have the best Quality of Recognition. In addition, because the method introduced in this thesis uses the histogram when calculating moments, the computational costs are orders of magnitude smaller than other descriptors discussed.

Future research into the computational complexity of these algorithms will better quantify their efficiency. Experiments with natural images are a logical next step for investigation as well. Additional translation, rotation, and scaling of objects can be added to improve comparisons between descriptors.

BIBLIOGRAPHY

[1] R.C. Gonzalez and R.E. Woods, *Digital Image Processing*, 3rd ed. Upper Saddle River: Prentice-Hall, 2008.

[2] R.A. Baggs and D.E. Tamir, "Non-rigid Image Registration", P*roceedings of the Florida Artificial Intelligence Research Symposium*, Coconut Grove, FL, 2008.

[3] D.E. Tamir, N. T. Shaked, W. J. Geerts, S. Dolev, "Compressive Sensing of Object-Signature", *Proceedings of the 3rd International Workshop on Optical Super Computing*, Bertinoro, Italy, 2010.

[4] L. Gupta and M.D. Srinath, "Contour sequence moments for the classification of closed planar shapes", *Pattern Recognition*, vol. 20, no. 3, pp. 267-272, June, 1987.

[5] P.L.E. Ekombo, N. Ennahnahi, M. Oumsis, M. Meknassi, "Application of affine invariant Fourier descriptor to shape-based image retrieval", *International Journal of Computer Science and Network Security*, vol. 9, no. 7, pp. 240-247, July, 2009.

[6] Y. Hu and Z. Li, "An Improved Shape Signature for Shape Representation and Image Retrieval", *Journal of Software*, vol. 8, no. 11, pp. 2925-2929, Nov., 2013.

[7] M.K. Hu, "Visual pattern recognition by moment invariants", *IRE Transactions on Information Theory*, vol. 8, Feb., 1962.

[8] E. Slud. (Spring 2009). "Scaled Relative Frequency Histograms" (lecture notes) [Online]. Available: http://www.math.umd.edu/~slud/s430/Handouts/Histogram.pdf.

[9] J. Flusser, T. Suk, B. Zitová., *Moments and Moment Invariants in Pattern Recognition*, Chichester, UK: John Wiley & Sons Ltd., 2009.

[10] M. Yang, K. Kpalma, R. Joseph, "A Survey of Shape Feature Extraction Techniques", *Pattern Recognition*, pp. 43-90, Nov., 2008.

[11] R.J. Prokop and A.P. Reeves "A survey of moment-based techniques for unoccluded object representation and recognition", *CVGIP: Graphics Models and Image Processing*, vol. 54, no. 5, pp. 438-460, Sept. 1992.

[12] C.C. Chen, "Improved moment invariants for shape discrimination", *Pattern Recognition*, vol. 26, pp. 683-686, May, 1993.

[13] L. Keyes and A. Winstanley, "Using moment invariants for classifying shapes on large-scale maps", *Computers, Environment and Urban Systems*, vol. 25, pp. 119-130, Jan., 2001.

[14] J. Žunić, “Shape Descriptors for Image Analysis”, *Zbornik Radova MI-SANU*, Vol. 15, pp. 5-38, 2012.

[15] M.K. Mandal, T. Aboulnasr, S. Panchanathan, “Image indexing using moments and wavelets”, *IEEE Transactions on Consumer Electronics.*, vol. 42, no. 3, pp. 557-565, Aug. 1996.

[16] J. Han and M. Kamber, *Data Mining: Concepts and Techniques*, 2nd ed. San Francisco: Morgan Kaufmann, 2006.